Thematic Topic: Alternative Fuels and Sustainability

14th U.S. National Combustion Meeting
Organized by the Eastern States Section of the Combustion Institute
March 16–19, 2025
Boston, Massachusetts

Effects of Heating Rate and Oxide Layer Growth on the Ignition of Iron Powder

Echo St. Germain[*]*, Randall Erb, Yiannis Levendis*

Mechanical and Industrial Engineering, Northeastern University, Boston, MA 02115, USA
[*]*Corresponding Author Email: gaugush.e@northeastern.edu*

Abstract: This manuscript reports on the combustion of pulverized iron, a promising but understudied alternative to fossil fuels. More needs to be understood about igniting and reducing the iron powder to maximize the efficiency of this fuel cycle. The specifics of iron ignition depend on many variables, one of which is the thickness of the oxide layer. A thick oxide layer may delay or altogether prevent ignition of particles and decrease fuel conversion efficiency. The work presented here aims to empirically determine how the heating rate and oxide layer of iron particles can inhibit ignition. These findings are then compared to simulations done by others on spherical particles with various oxide layer thickness. To accomplish this, two differently sized populations of irregularly shaped iron particles (38 μm and 45 μm) are inserted into an externally heated drop tube furnace, operated at wall temperatures between 1000K - 1200K with various air flow rates. Hence, these iron particles experience different temperature profiles and oxidation rates while falling through the furnace, forming oxide layers, and sometimes reaching their ignition temperature. The probability of particles igniting is calculated based on the shape of the final oxidized particle. In separate experiments, iron particles that are treated to exhibit significant preexisting oxide layers are also put through the furnace to better understand how an oxide shell inhibits ignition. The results of these experiments will be used in future work to determine ranges of ignition temperature based on the heating rate and oxide thickness to outline conditions which can be followed for successful iron particle ignition. Additionally, by understanding the acceptable degree of pre-oxidation for set furnace conditions, requirements can be created for the maximum humidity and temperature conditions at which iron particles can be stored.

Keywords: Iron Powder, Fuel Cycle, Oxide Layer

1. Introduction

Rapid decarbonization of energy is critical to minimize the long-term effects of greenhouse gases (GHG) on the climate. Globally transitioning to new methods of energy generation has many challenges that make such a task difficult. Carbon based fuels have become a staple of many economies, while newer energy sources such as solar and wind power require new investments in infrastructure. Additionally, as the world becomes more populated and reliant on modern technologies, the demand for energy is increasing. Currently, CO_2 makes up the largest portion of GHG emissions with the largest contributions to CO_2 coming from power generation, industrial combustion, and transportation industries [1]. Worldwide a significant portion of this CO_2 is a result of coal combustion. While some countries have transitioned away from coal, this is often at the cost of switching to natural gas, as seen in the United States [2]. Coal remains popular due to its abundance, affordability, and historical importance to growing economies; increasing the difficulty of transitioning away from coal in countries such as in India [3] and China [4]. Due to how ingrained coal as a fuel source is to many economies, an alternative fuel which is as similar as possible to coal is important to aid in global decarbonization while allowing countries to continue increasing their energy usage. Additionally, fuel which can be used with existing coal

power plants could be less disruptive to local economies and workforces, helping smooth the transition.

Currently hydrogen[5], ammonia[6], and metal powders [7] are the main alternative fuels that can be used in combustion without producing CO_2. Out of these fuels metal powder, specifically iron, is an attractive replacement to coal. Iron is abundant, has a similar volumetric energy density as coal, and could be used in retrofitted coal-fired plants[8]. Retrofitting coal power plants into iron power plants would reduce both GHG and pollutants while keeping the plants operating, maintaining some similar local employment opportunities and increasing the chance that iron retrofitting would be approved. While iron is initially more costly than coal it can be ignited and burned multiple times. When iron ignites it turns into iron oxides, which can be reduced back into iron using any iron reduction method using hydrogen [9-11], which can be done by transporting the iron oxides to hydrogen production plants. This recyclability would allow the iron to be used as a fuel, storing energy chemically with the reduction process that can be later released to heat boilers at power plants. For iron to replace coal, the combustion properties of iron need to be fully understood so power plants can be retrofitted to maximize the production of usable energy.

Research into iron ignition for fuel has been initiated relatively recently. To understand combustion properties such as burn time and temperature profiles, multiple research groups have examined iron ignition using laser ignition [12, 13], elevated gas temperatures [14, 15], and simulations to predict additional properties of iron combustion [16, 17]. The ignition temperature of iron can depend on many variables, such as particle size, shape, and preexisting oxide layer, as described in recent experimental [18, 19] and computational papers [20]. The inhibition of iron combustion due to the presence of a solid oxide layer on the particles provides additional challenges to iron ignition which most fuels do not share. The formation and presence of iron oxides on iron powders is important to understand how to guarantee complete combustion of iron, improving the fuel conversion efficiency of iron powder.

There are two main ways an oxide layer can form on an iron particle before ignition. First, humid storage conditions can result in iron rusting before reaching the furnace. Understanding how humidity-driven oxidation of iron inhibits ignition is particularly important if iron fuel is to be used in maritime operations, a potential application of iron fuel [21] where the powder may be exposed to humid and salty air if not properly stored. Second, maintaining a particle at elevated temperatures for too long before reaching the ignition temperature can also result in significant oxidation. While dry iron is normally stable, particles reach elevated temperatures while being injected into furnaces. If this happens gradually the outside of the iron may oxidize too slowly to kickstart ignition but fast enough to create a significant layer separating the iron core from the external oxygen. Simulations by Mi et al. [20] show that an oxide layer as thin as 0.3% of the particle diameter can have a significant increase on the ignition temperature of 1-50 μm iron particles. To our knowledge, no empirical results on the effects of an oxide layer have yet been reported.

This research aims to provide empirical results about how the presence of oxide layers due to humidity and prolonged heating in a furnace can change the behavior of iron ignition. This investigation is primarily conducted by introducing iron particles into the vertical tube furnace in a flow of room temperature air, which gradually heats up in the furnace as the particle falls. By creating various heating rates iron particles can be driven to significantly oxidize before reaching the ignition temperature. Oxidation due to particles being left in humid conditions, in this case through water submersion, is also examined to investigate the sensitivity of the iron powder to thin

oxide layers formed at relatively cool temperatures.

2. Experimental

Irregularly shaped iron powder from *Metal Powder USA* was sieved and separated into two populations: iron particles larger than 45 µm, and iron particles smaller than 38 µm. Their images, shown in Fig. 1, were captured using an *Olympus* BX51 Fluorescence optical microscope so that changes in particle color could be examined.

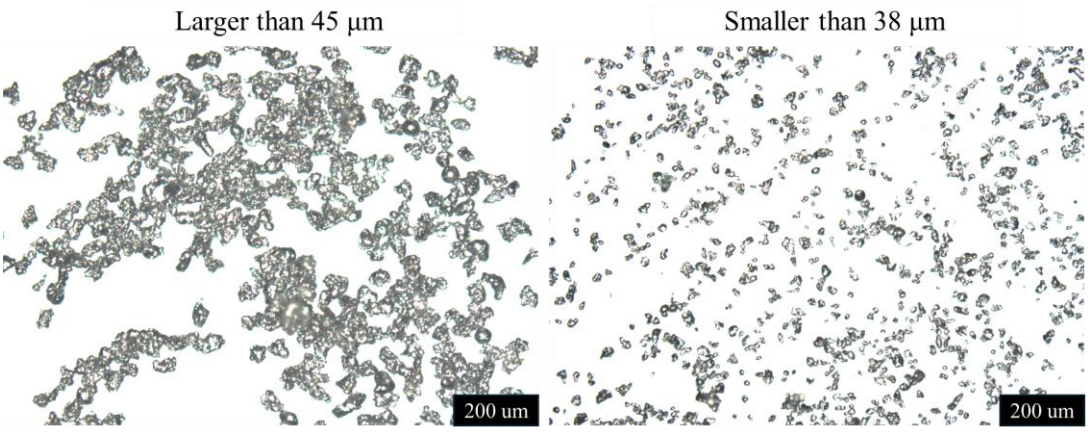

Fig. 1. Iron particles from *Metal Powder USA* before ignition or pre-oxidation.

For each experiment iron powder was inserted into a plastic tube, which was attached to a *Harvard Instruments* syringe pump and was vibrated to fluidize the particles. A stream of air at 1 L/min was channeled into the vibrating tube, pushing the iron powder up and into a feeding tube. This method provided a consistent flow of iron into the top of an *ATS* electrically-heated drop-tube furnace, through a stainless-steel water-cooled injector. To manipulate the temperature profile within the furnace, while maintaining a similar maximum temperature, additional air was pumped into the top of the furnace, concentrically to the injector air as depicted in Fig 2. This additional air was inserted at a rate of 1 L/min, 2L/min and 5L/min, resulting in net airflows of 1L/min, 2L/min, 3L/min and 6L/min for the various experiments.

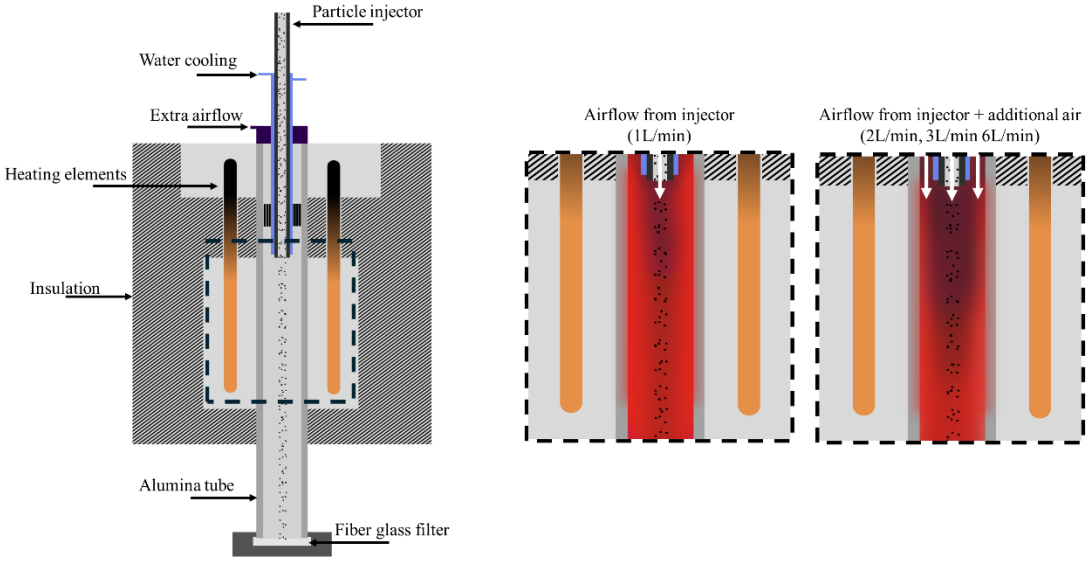

Fig. 2. Diagram of the drop tube furnace and example of how the temperature profile within the tube changes when additional airflow is introduced.

After falling through the furnace, particles were collected on a fiber glass filter. This was done for four furnace wall temperatures, T_{wall}, of 1000K, 1050K, 1100K, and 1200K for the four different air flow rates with both populations of small and large iron particles. Two sets of experiments were also done using the small and large particles which were submerged in 60°C water overnight to form oxide layers. These particles were then injected into the furnace at the minimum airflow, 1L/min, at temperatures where ignition would normally be expected. Faster airflow resulted in more gradual heating rates for the iron particles, since more room temperature air was being introduced to the furnace bringing down the temperature near the furnace inlet. A coarse temperature profile of the center gas temperature, T_{gas}. at various heights within the furnace was collected using a 56 cm long K-type thermocouple rod (manufactured by *Omega*), inserted through the furnace until reaching the elevation of the heating elements. The measured temperatures, shown in Fig 3, were corrected for radiation effects following the procedure outlined in previous experiments using this setup [22].

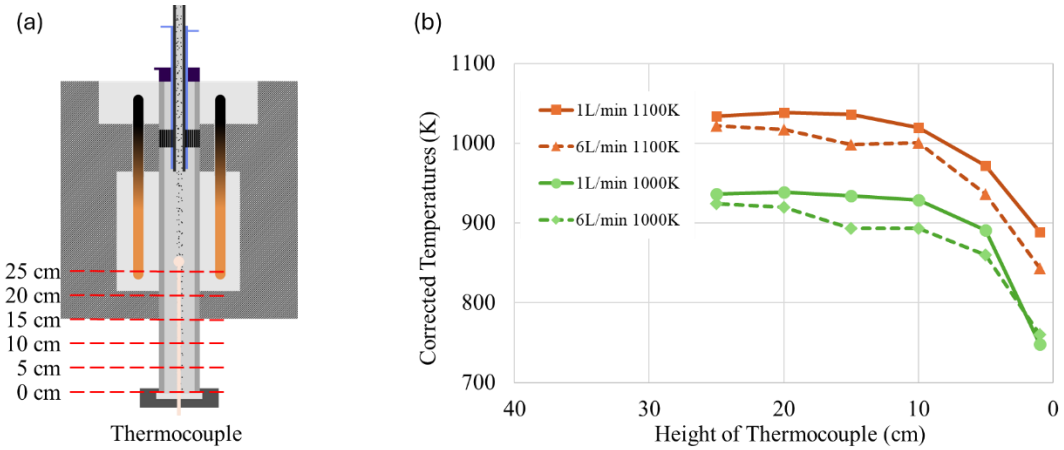

Fig. 3. (a) Schematic of the furnace indicating the measured locations of the thermocouple. (b) Temperature profiles gathered by the thermocouple measurement during the minimum and maximum flow rates for T_{wall}=1000K and T_{wall}=1100K along the furnace height.

The temperature profiles plotted in Fig. 3b correspond to the height-dependent centerline temperatures of the tube furnace with T_{wall}=1000K and T_{wall}=1100K. They show that while forced air flow prevents the gas within the furnace from reaching the wall temperature set point during experiments, particles are subjected to similar peak oven temperatures for the different tested flow rates. The peak oven temperatures tend to be 75K lower than the furnace set temperature near the centerline of the tube. Temperature within the heating element zone is expected to be constant and is not documented as accurately due to the top of the thermocouple rod experiencing lateral movement when fully extended with the high air flow. Based on preliminary observations, the gas near the injector tip is cooler during higher airflow rates, mirroring the profile at the bottom of the furnace resulting in a more gradual increase of T_{gas}. Additional measurements are required to validate the furnace temperature near where the particles are injected.

3. Results and Discussion

Particles from all experiments were collected at the exit of the furnace and imaged using an optical microscope. By looking at the overall shape of the collected oxidized particles, the percentage of iron particles that ignited could be determined. Nonspherical particles remained unignited while spherical particles ignited, melted, spherodized due to surface tension and then resolidified, shown in Fig 4. Additionally, all particles appeared visually darker and less shiny after falling through the

furnace compared to their original state. This indicates that all the particles formed a visible layer of Fe_3O_4, which absorbs incident light and appears as a darker color than pure iron which is shiny and reflective. Particles which experienced higher furnace temperatures were also coated with some orange clumps of powder, a signifier that Fe_2O_3 nanoparticles formed upon ignition.

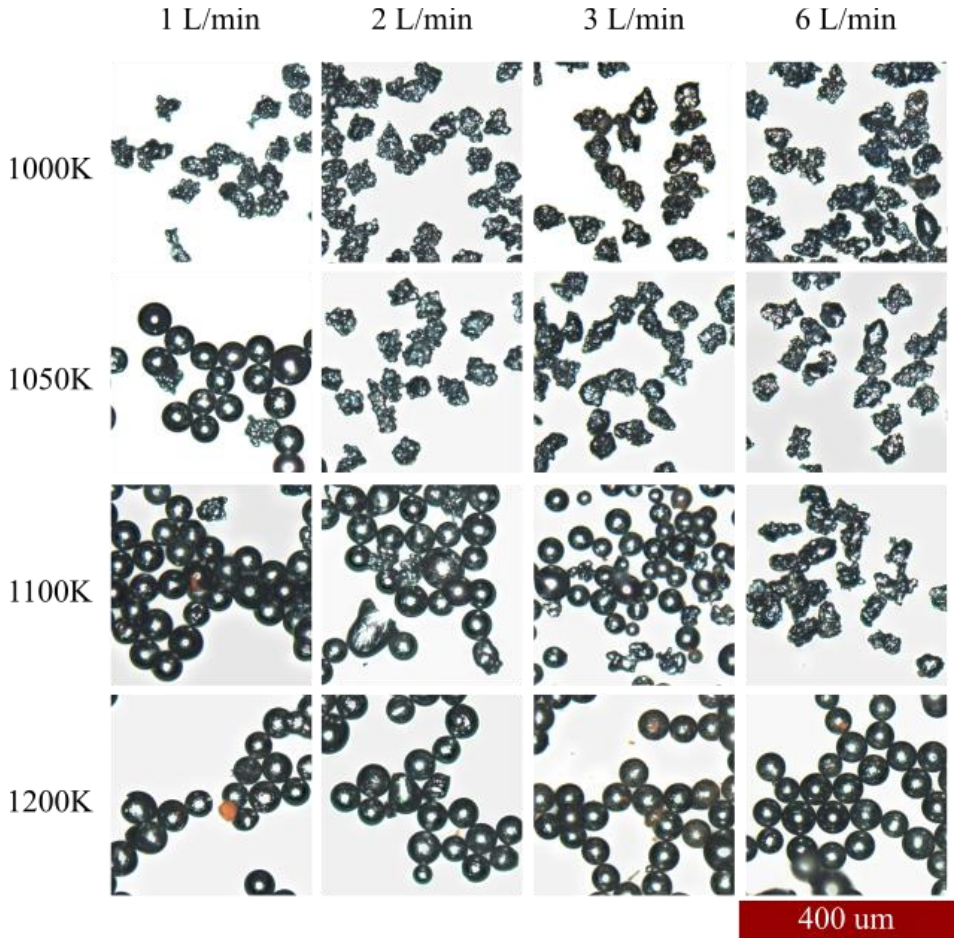

Fig. 4. Micrographs of large particles after going through the furnace with various airflows. Displayed temperatures correspond to T_{wall}. Particles that underwent ignition melted and spherodized before collection.

Accounting for the actual temperature profile, Figure 4 shows that at 1L/min the large particles ignite around T_{wall} = 1050K (T_{gas} = 975K) and at 2L/min and 3L/min they start to ignite around T_{wall} = 1100K (T_{gas} = 1025K), and at 6L/min particles don't start to ignite until after T_{wall} = 1100K (T_{gas} = 1025K). The same trend is followed by the population of smaller particles; however, the percentage of particles that ignite for the smaller size is consistently lower, as shown in Fig 5. Since the thickness of the natural oxide layer is expected to be the same for both particle sizes, a greater overall volume of the small particles is pre-oxidized compared to the larger particles due to the higher surface area to volume ratio. This may explain the decrease in ignition probability for the smaller particles, even during the low airflow rate, as there is a smaller volume of iron directly under the oxide layer which can quickly react and start releasing energy. In addition, smaller particles tend to equilibrate faster with the environment which removes heat during the oxidation process.

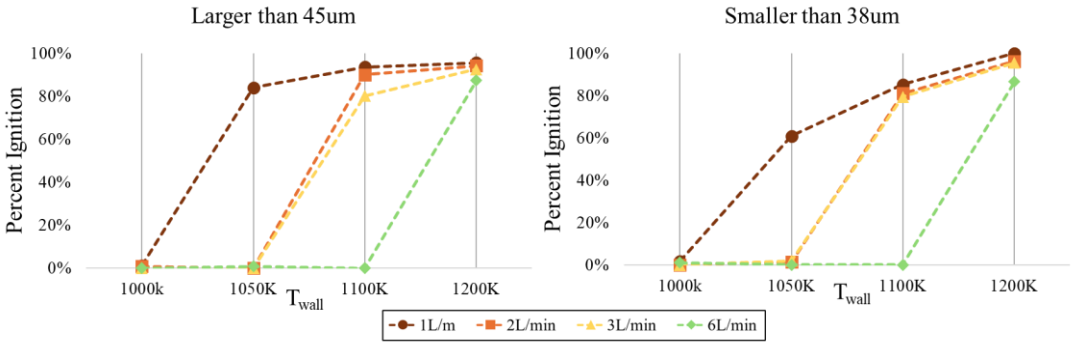

Fig. 5. Percentage of large and small particles that ignited at T_{wall} with various airflow rates.

Examination of the particles under Electron Dispersive Spectroscopy (EDS), using a *TESCAN VEGA 3 LMU* Scanning Electron Microscope (SEM) helps provide an understanding of the oxide layer. Both the original oxide layer and the layer that is formed when particles go through the furnace with higher airflow are too thin to discern using EDS. However, the oxide layer that forms during the lower 1L/min airflow rate is noticeable. Fig. 6 shows the difference between two sets of small particles, one that went through a furnace where T_{wall} = 1050K with 1L/min of air flow and one that went through a furnace where T_{wall} = 1050K with 6L/min of air flow. The sample with 1L/min air flow has an oxide layer thickness of approximately 1.5 μm for unignited particles, while the oxide layer for the 6L/min particles is smaller than the 0.5 μm resolution of the EDS scan. The 1L/min oxide layer may be thicker because the particle is subjected to higher temperatures that are still below the ignition temperature.

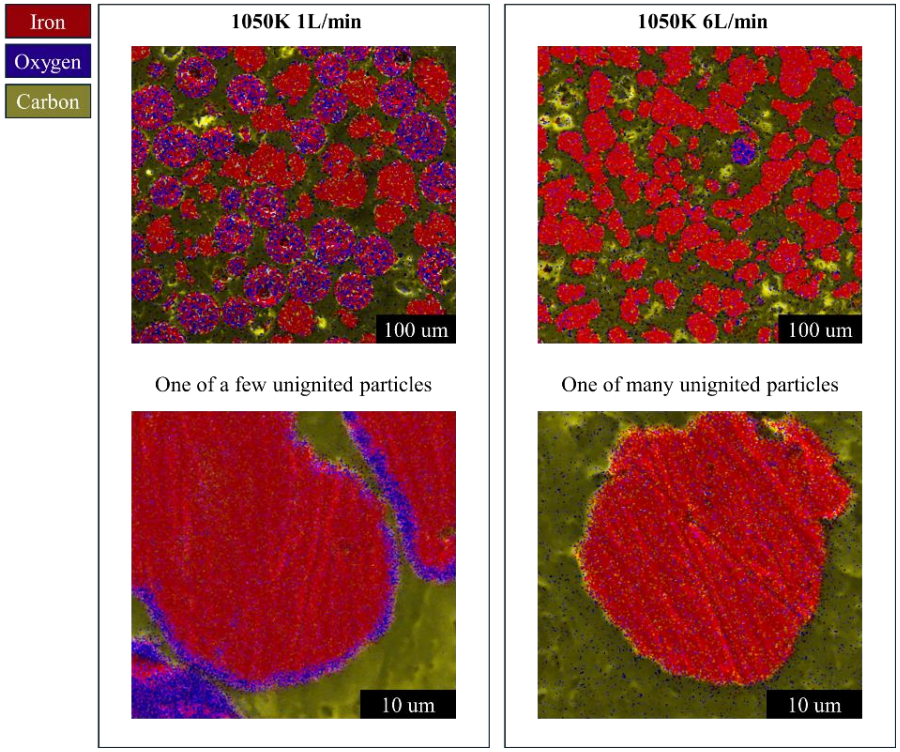

Fig. 6. False-colored EDS micrographs of iron powder after falling through the drop tube furnace where T_{wall} = 1050K at flowrates of 1L/min and 6L/min. Here, red, blue, and yellow indicate the existence of iron, oxygen, and carbon respectively detected by EDS. Iron oxide therefore appears purple.

The unusually thick oxide layer from the 1L/min samples is also thicker than the oxide layer of particles that were oxidized in water, which did not have large enough oxidation layers to be detected with EDS. However, using an optical microscope shows that the color and shine of the submerged particles changed, indicating the presence of Fe_3O_4 on the surfaces of the particles and flakes of Fe_2O_3 adhered to the larger particles as shown in Fig 7. This small oxide layer seems to have been sufficient to reduce the likelihood of particle ignition. Particles with where T_{wall} = 1050K and a flow rate of 1L/min without pre-oxidation ignited about 84% of the time, but particles that were soaked in water overnight only ignited around 61% of the time.

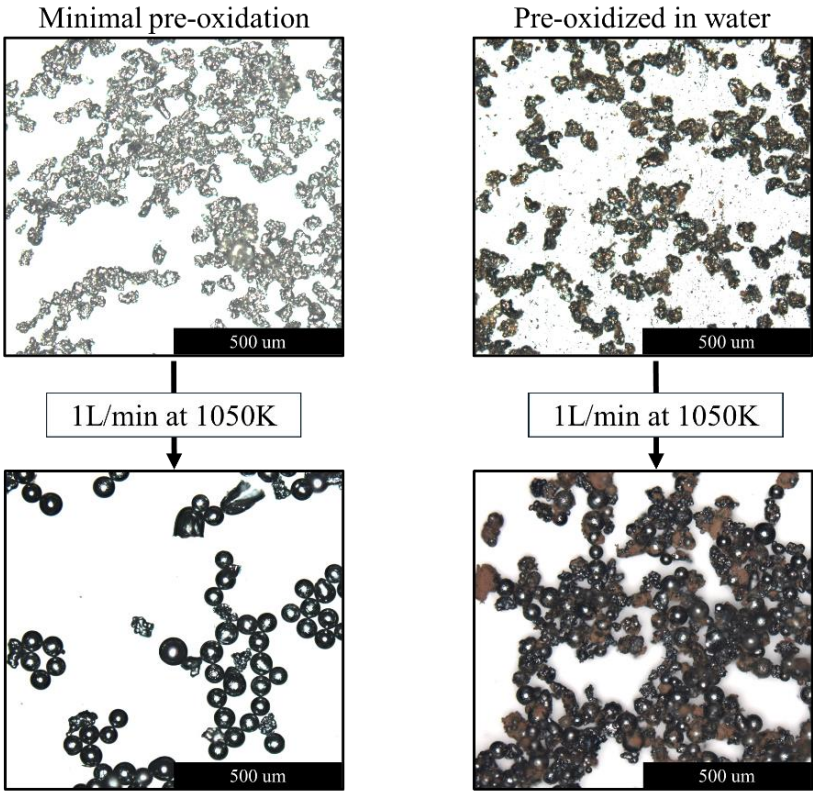

Fig. 7. Optical micrographs of iron particles before and after traveling through the furnace with T_{wall} = 1050K and a net air flow rate of 1L/min.

These results together show preliminary evidence that it does not require a large oxide layer to compromise the ignition propensity of iron particles. Further, such an oxide layer may be formed while a particle is traveling into the center of the furnace. Simulations by Mi et al. [20] show that there is a significant change in predicted particle ignition temperature when accounting for an oxide layer of just 1 nm compared to simulations without an oxide layer effect. This is likely because the diffusion of oxygen is limited by the reduced molecular diffusivity of iron oxide relative to iron. Simulations show that oxide layers below 0.3% of the total particle diameter have similar ignition temperatures but once this percentage increases past the 0.3% threshold the ignition properties of iron begin to significantly shift, requiring higher temperatures for ignition. This requirement is important to consider for iron as a fuel source, since when iron particles fall through a furnace, they experience some degree of heating up before reaching ignition temperature, resulting in the normally thin oxide layer growing potentially rapidly. This growth can also occur if the iron particle is exposed to humid conditions which can cause a surface layer of rust to form. Therefore, if a significant oxide layer is present before reaching the ignition temperature the solid oxide layer can act as a barrier, inhibiting further oxidation and ignition of the iron particles.

Based on simulations showing 0.3% oxide thickness as the crossover between ignition characteristics, the iron powder used in these studies should have consistent ignition properties if their oxide layer is under 100nm. This value may be lower, since the simulations by Mi et al. [20] used spherical particles and this research uses irregularly shaped iron particles with a larger surface area ratio. Examining oxide thickness to this degree of accuracy is challenging, oxide layers under 500 nm do not clearly show up in EDS. Observable color change can be observed for oxide layers that have grown past just 25nm thickness [23]. Color change is clearly observed in powders subjected to water immersion and in powders inserted into the furnace even in cases where ignition was not observed.

Particles that experienced a more gradual increase in furnace temperature due to additional airflow in the furnace required a gas temperature of at least 50K higher to ignite, compared to those which quickly reached the maximum gas temperature before having time to form an oxide layer. Practically, this means that ovens or furnaces being used to ignite iron for fuel need to keep the particles cool right until they reach the desired ignition location, or else they risk the iron pre-oxidizing while entering the furnace and becoming less likely to ignite. Additionally, particles which were submerged in water to form a thin oxide layer ignited at a reduced rate (23% less) than non-oxidized particles. If particles are stored in humid environments for significant periods of time this too can result in oxidized iron that exhibits reduced ignition behavior, decreasing the efficiency of such iron powders as a fuel.

4. Conclusions

This work shows how even an oxide layer between 25 and 500nm can significantly raise the ignition temperature and reduce the ignition probability of iron particles. This can occur if the oxide layer is formed due to storage of the iron powder under humid conditions or a gradual heating of the powder prior to reaching the required ignition temperature. Overall, the use of iron powder as an energy source will require care to avoid the unintended formation of oxide layers prior to ignition. Future studies will seek to characterize the role played by sub-micron oxide thicknesses as well as to investigate the ignition of reduced particles. Reduced particles retain a spherical shape but potentially have a large surface area ratio due to surface deformations during the reduction process. These changes in particle morphology may change how susceptible the particle ignition temperature is based on oxide layer thickness.

5. Acknowledgements

This work was supported by the US National Science Foundation Grant # DMR-G00008208.

6. References

[1] M. Filonchyk, M. P. Peterson, H. Yan, A. Gusev, L. Zhang, Y. He, and S. Yang, "Greenhouse gas emissions and reduction strategies for the world's largest greenhouse gas emitters," *Sci Total Environ*, vol. 944, p. 173895, Sep 20 2024, doi: 10.1016/j.scitotenv.2024.173895.
[2] J. A. Burney, "The downstream air pollution impacts of the transition from coal to natural gas in the United States," *Nature Sustainability*, vol. 3, no. 2, pp. 152-160, 2020, doi: 10.1038/s41893-019-0453-5.
[3] L. Montrone, N. Ohlendorf, and R. Chandra, "The political economy of coal in India – Evidence from expert interviews," *Energy for Sustainable Development*, vol. 61, pp. 230-240, 2021, doi: 10.1016/j.esd.2021.02.003.
[4] L. Shen, T.-m. Gao, and X. Cheng, "China's coal policy since 1979: A brief overview," *Energy Policy*, 2011, doi: 10.1016/j.enpol.2011.10.001.
[5] M. A. Habib, G. A. Q. Abdulrahman, A. B. S. Alquaity, and N. A. A. Qasem, "Hydrogen

combustion, production, and applications: A review," *Alexandria Engineering Journal*, vol. 100, pp. 182-207, 2024, doi: 10.1016/j.aej.2024.05.030.
[6] L. Kang, W. Pan, J. Zhang, W. Wang, and C. Tang, "A review on ammonia blends combustion for industrial applications," *Fuel*, vol. 332, 2023, doi: 10.1016/j.fuel.2022.126150.
[7] J. M. Bergthorson, S. Goroshin, M. J. Soo, P. Julien, J. Palecka, D. L. Frost, and D. J. Jarvis, "Direct combustion of recyclable metal fuels for zero-carbon heat and power," *Applied Energy*, vol. 160, pp. 368-382, 2015, doi: 10.1016/j.apenergy.2015.09.037.
[8] J. Janicka, P. Debiagi, A. Scholtissek, A. Dreizler, B. Epple, R. Pawellek, A. Maltsev, and C. Hasse, "The potential of retrofitting existing coal power plants: A case study for operation with green iron," *Applied Energy*, vol. 339, 2023, doi: 10.1016/j.apenergy.2023.120950.
[9] J. M. Bergthorson, "Recyclable metal fuels for clean and compact zero-carbon power," *Progress in Energy and Combustion Science*, vol. 68, pp. 169-196, 2018, doi: 10.1016/j.pecs.2018.05.001.
[10] N. C. Stevens, W. Prasidha, N. G. Deen, L. Meeuwsen, M. Baigmohammadi, Y. Shoshin, L. P. H. de Goey, and G. Finotello, "Cyclic reduction of combusted iron powder: A study on the material properties and conversion reaction in the iron fuel cycle," *Powder Technology*, vol. 441, 2024, doi: 10.1016/j.powtec.2024.119786.
[11] L. Choisez, K. Hemke, Ö. Özgün, C. Pistidda, H. Jeppesen, D. Raabe, and Y. Ma, "Hydrogen-based direct reduction of combusted iron powder: Deep pre-oxidation, reduction kinetics and microstructural analysis," *Acta Materialia*, vol. 268, 2024, doi: 10.1016/j.actamat.2024.119752.
[12] D. Ning, Y. Shoshin, J. A. van Oijen, G. Finotello, and L. P. H. de Goey, "Burn time and combustion regime of laser-ignited single iron particle," *Combustion and Flame*, vol. 230, 2021, doi: 10.1016/j.combustflame.2021.111424.
[13] D. Ning, Y. Shoshin, M. van Stiphout, J. van Oijen, G. Finotello, and P. de Goey, "Temperature and phase transitions of laser-ignited single iron particle," *Combustion and Flame*, vol. 236, 2022, doi: 10.1016/j.combustflame.2021.111801.
[14] S. Li, J. Huang, W. Weng, Y. Qian, X. Lu, M. Aldén, and Z. Li, "Ignition and combustion behavior of single micron-sized iron particle in hot gas flow," *Combustion and Flame*, vol. 241, 2022, doi: 10.1016/j.combustflame.2022.112099.
[15] A. Panahi, D. Chang, M. Schiemann, A. Fujinawa, X. Mi, J. M. Bergthorson, and Y. A. Levendis, "Combustion behavior of single iron particles-part I: An experimental study in a drop-tube furnace under high heating rates and high temperatures," *Applications in Energy and Combustion Science*, vol. 13, 2023, doi: 10.1016/j.jaecs.2022.100097.
[16] A. Fujinawa, L. C. Thijs, J. Jean-Philyppe, A. Panahi, D. Chang, M. Schiemann, Y. A. Levendis, J. M. Bergthorson, and X. Mi, "Combustion behavior of single iron particles, Part II: A theoretical analysis based on a zero-dimensional model," *Applications in Energy and Combustion Science*, vol. 14, 2023, doi: 10.1016/j.jaecs.2023.100145.
[17] J. Jean-Philyppe, A. Fujinawa, J. M. Bergthorson, and X. Mi, "The ignition of fine iron particles in the Knudsen transition regime," *Combustion and Flame*, vol. 255, 2023, doi: 10.1016/j.combustflame.2023.112869.
[18] M. Abdallah, Y. Shoshin, G. Finotello, and L. P. H. de Goey, "Iron particles ignition in different hot coflow temperatures," *Proceedings of the Combustion Institute*, vol. 40, no. 1-4, 2024, doi: 10.1016/j.proci.2024.105261.
[19] D. Ning, Y. Li, T. Li, B. Böhm, and A. Dreizler, "Size-resolved ignition temperatures of isolated iron microparticles," *Combustion and Flame*, vol. 270, 2024, doi: 10.1016/j.combustflame.2024.113779.
[20] X. Mi, A. Fujinawa, and J. M. Bergthorson, "A quantitative analysis of the ignition characteristics of fine iron particles," *Combustion and Flame*, vol. 240, 2022, doi: 10.1016/j.combustflame.2022.112011.
[21] J. de Kwant, R. Hekkenberg, A. Souflis-Rigas, and A. A. Kana, "Exploring the potential of iron powder as fuel on the design and performance of container ships," *International Shipbuilding Progress*, vol. 70, no. 1, pp. 3-28, 2023, doi: 10.3233/isp-220012.
[22] R. Khatami, C. Stivers, and Y. A. Levendis, "Ignition characteristics of single coal particles from three different ranks in O2/N2 and O2/CO2 atmospheres," *Combustion and Flame*, vol. 159, no. 12, pp.

3554-3568, 2012, doi: 10.1016/j.combustflame.2012.06.019.
[23] V. Goossens, J. Wielant, S. Van Gils, R. Finsy, and H. Terryn, "Optical properties of thin iron oxide films on steel," *Surface and Interface Analysis,* vol. 38, no. 4, pp. 489-493, 2006, doi: 10.1002/sia.2219.